

X-Ray Study of the Cation Distribution in the Ternary Oxide, $6 \text{Bi}_2\text{O}_3\text{-V}_2\text{O}_5$

S. Kashida and T. Hori

Department of Physics, Niigata University, Ikarashi, Niigata, 950-21, Japan

Received June 5, 1995; in revised form December 13, 1995; accepted December 14, 1995

The structure of the ternary oxide $6 \text{Bi}_2\text{O}_3\text{-V}_2\text{O}_5$ has been investigated using single crystal X-ray diffraction data. It has a fluorite-type superstructure with a pseudo monoclinic cell, $a = 20.023 \text{ \AA}$, $b = 11.668 \text{ \AA}$, $c = 20.472 \text{ \AA}$, and $\beta = 107.13^\circ$, (the relation to the fluorite subcell is $a \approx 3/2[1, 1, 2]_c$, $b \approx 3/2[1, 1, 0]_c$, and $c \approx 1/2[5, 5, 2]_c$), but the real crystal symmetry is $P1$. The positions of metal atoms are refined to $R = 0.12$. The structure is characterized by six cation layers along the c axis, each containing 18 metal atoms. The cation arrangement can be represented using the numbers of V atoms as 4–0–4–4–0–4. Along the b axis, the crystal has square wave type displacements ($\approx 0.6 \text{ \AA}$). The origin of this large distortion is attributed to the Coulomb repulsion between V atoms in the nearest neighbor sites. © 1996 Academic Press, Inc.

INTRODUCTION

Bismuth sesquioxide behaves as a good ionic conductor in its high temperature cubic fluorite phase. This compound forms solid solutions with many other metal oxides. If alkaline earth oxides (CaO, SrO, or BaO) are added the compounds have rhombohedral layer structures, and if transition metal oxides (V_2O_5 , Nb_2O_5 , Ta_2O_5 , or Y_2O_3) are added they have fluorite-like structures. Recent electron diffraction and high resolution electron microscopic studies have disclosed a variety of superstructures in the so-called "stabilized bismuth oxides" (1–7).

Among the mixed bismuth oxides, the $\text{Bi}_2\text{O}_3\text{-V}_2\text{O}_5$ system has been studied most widely, by electron diffraction (5, 7), Raman and ^{51}V NMR spectroscopies (8), and X-ray diffraction (9). These studies showed that the 9:1 compound has a $3 \times 3 \times 3$ superstructure derived from the fluorite lattice, designated as type I (Fig. 1) (5). In this type I, the minority atoms (V) are located at every third layer along the $[111]_c$ axis (the subscript c means the prototypic cubic fluorite cell). Vanadium atoms occupy the third neighbor sites of the cation lattice, and oxygen vacancies are concentrated at nearest neighbor sites of V atoms (9).

The structure of the mixed oxides changes with the con-

tent of added vanadium atoms. When the number of V atoms increases from 9:1, it is no longer possible to retain the type I structure, and some of the Bi atoms between the vanadium layers will be replaced by V atoms. In recent electron diffraction studies, Zhou reported that the 6:1 compounds have structure types designated as types IIa–IIc (5, 7). He has proposed a model structure which is composed of V_4O_{10} tetrahedral clusters. However, details of the structure are not given yet. The aim of the present study is to determine this structure. Single crystal samples were grown with the composition of 6:1, and X-ray diffraction data were collected at room temperature using a four-circle diffractometer.

EXPERIMENTAL

Crystal samples of $6 \text{Bi}_2\text{O}_3\text{-V}_2\text{O}_5$ have been prepared by melting. Details of the procedure are identical to those reported previously (5, 9). The samples were transparent yellow and showed clear cleavage. From X-ray studies, the cleavage was found to be along the a – b or the $(111)_c$ plane. In the polarization microscopic observation, the samples showed clear extinction suggesting that the crystal is anisotropic. This is in contrast to the case of the 9:1 compound which does not show any clear cleavage or extinction (9).

The crystal symmetry and approximate unit cell parameters were determined from precession photographs (see Fig. 2). The observed strong reflections show that the crystal is composed of fluorite-like subcells. Superlattice reflections are observed at $1/6$ along one of the $[111]_c$ directions. The diffraction pattern is closely related to that of type IIa reported by Zhou (5, 7). The unit cell vectors in the reciprocal space can be taken as

$$\begin{aligned} \mathbf{a}_m^* &\approx 1/18 \mathbf{a}_c^* + 1/18 \mathbf{b}_c^* + 5/18 \mathbf{c}_c^* \\ \mathbf{b}_m^* &\approx -1/3 \mathbf{a}_c^* + 1/3 \mathbf{b}_c^* \\ \mathbf{c}_m^* &\approx -1/6 \mathbf{a}_c^* - 1/6 \mathbf{b}_c^* + 1/6 \mathbf{c}_c^*, \end{aligned} \quad [1]$$

where \mathbf{a}_c^* , \mathbf{b}_c^* , and \mathbf{c}_c^* are the reciprocal unit cell vectors of the prototypic cubic fluorite cell. The deduced real unit cell vectors are

$$\begin{aligned} \mathbf{a}_m &\approx 3/2 \mathbf{a}_c + 3/2 \mathbf{b}_c + 3 \mathbf{c}_c \\ \mathbf{b}_m &\approx -3/2 \mathbf{a}_c + 3/2 \mathbf{b}_c \\ \mathbf{c}_m &\approx -5/2 \mathbf{a}_c - 5/2 \mathbf{b}_c + \mathbf{c}_c. \end{aligned} \quad [2]$$

Here, we have taken the monoclinic unit cell (see Fig. 3). The relation to the triclinic unit cell (\mathbf{a}_t , \mathbf{b}_t , \mathbf{c}_t) proposed by Zhou for type IIa (5, 7) is

$$\begin{aligned} \mathbf{a}_m &\approx \mathbf{a}_t + \mathbf{b}_t \\ \mathbf{b}_m &\approx -\mathbf{a}_t + \mathbf{b}_t \\ \mathbf{c}_m &\approx \mathbf{a}_t + \mathbf{c}_t. \end{aligned} \quad [3]$$

The unit cell lengths are represented, using the prototypic fcc lattice parameter a_c , as $a_m = 3\sqrt{6}/2 a_c$, $b_m = 3\sqrt{2}/2 a_c$, and $c_m = a_m$. In this type IIa (following Zhou, we call this phase type IIa), the lattice is elongated along the c axis and contracted along the a axis ($c/a = 1.022$ and $a/b = 1.716 < \sqrt{3}$). The monoclinic angle changes from $\beta_0 = \cos^{-1}(1/3) = 109.47^\circ$ to 107.13° ($\Delta\beta \approx -2.1^\circ$).

After examining several different samples, we found that the $[010]$ zone diffraction pattern (Fig. 2a) always suffered

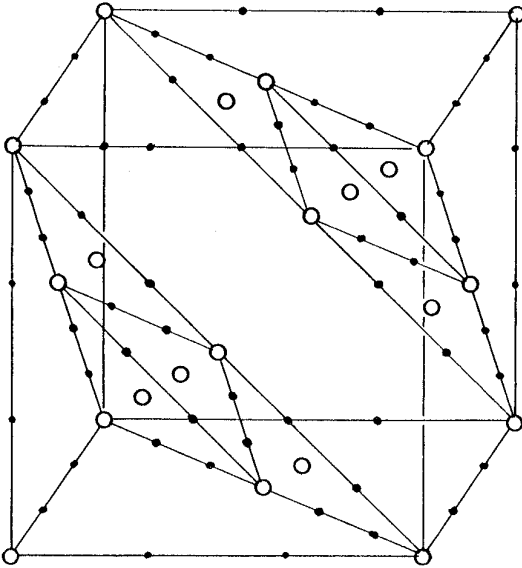


FIG. 1. The cation distribution in the $3 \times 3 \times 3$ superstructure of 9 Bi₂O₃-V₂O₅. Minority atoms (V) are represented by open circles and majority atoms (Bi) by black dots. For clarity, only some of the majority atoms are drawn. Note that V atoms occupy every third layers along the $[111]_c$ axis.

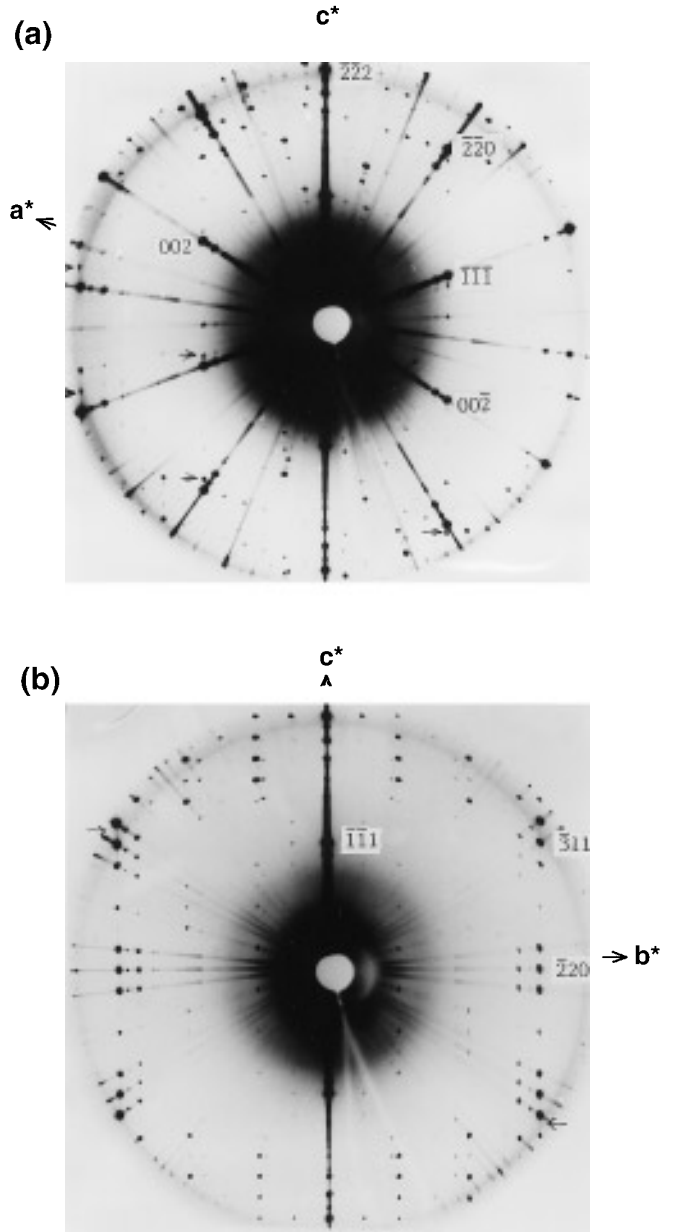


FIG. 2. Precession photographs of the type IIa structure, (a) the $[110]_c$ zone, (b) the $[112]_c$ zone. The pseudo-cubic indexing is used. The monoclinic reciprocal vectors are represented by a^* , b^* , and c^* . The ghosts due to the 120 twins and diffuse streaks are shown by arrows.

from contamination due to twins whose $\mathbf{a}\mathbf{b}$ axes are rotated $+120^\circ$ or -120° around the \mathbf{c}^* axis. In the crystal which we have used for data collection, faint ghosts are also discernible in X-ray photographs.

The intensity data were collected on a Huber four-circle diffractometer and graphite monochromated MoK α radiation was used. The data were collected in a hemisphere of the reciprocal space. Since it turned out that the cleaved

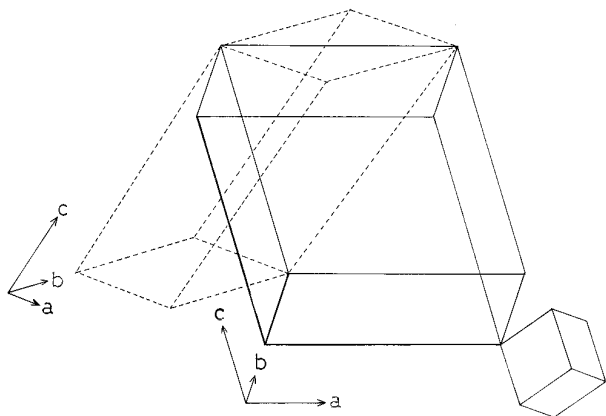


FIG. 3. The unit cell vectors of $6\text{Bi}_2\text{O}_3 \cdot \text{V}_2\text{O}_5$. The solid lines show the monoclinic unit cell. The dotted lines show the triclinic unit cell proposed by Zhou, and the cube shows the fluorite subcell.

crystals are very sensitive to mechanical stress, the sample was not ground into a sphere. The diffraction data were corrected for L_p factors. The crystal has a very large absorption coefficient and the correction was made for absorption by numerical integration. In Table 1, the crystal data and details of the data collection and refinements are given.

STRUCTURE DETERMINATION

The calculated Patterson maps showed an fcc-like array of heavy atoms. The maps also showed that the atoms with coordinates $|z| > 1/4$ have large displacements along the b axis, relative to those with $|z| < 1/4$. The solution of the

TABLE 1
Crystal and Reflection Data

Space group	$P\bar{1}$
Chemical formula	$\text{Bi}_{46}\text{V}_8\text{O}_{89}$, $Z = 2$
Lattice parameters (\AA , deg.)	$a = 20.023(29)$, $\alpha = 90.0(1)$ $b = 11.668(14)$, $\beta = 107.13(7)$ $c = 20.472(27)$, $\gamma = 90.0(1)$
Volume (\AA^3)	4570
D_{calc} (g/cm^3)	8.37
Absorption coefficient (cm^{-1})	856
Crystal size	$0.030 \times 0.027 \times 0.018 \text{ cm}^3$
Scan mode	$\omega/2\theta$
2θ max (deg)	60
Range in indices	$0 \leq h \leq 26$, $0 \leq k \leq 16$, $-27 \leq l \leq 27$
No. of reflections measured	25485
No. of reflections used in refinement	3264 ($I > 2\sigma(I)$)
No. of parameters refined	217
$R = \sum (F_o - F_c) / \sum F_o $	0.12

structure was searched for by starting from a regular array of metal atoms in the fcc lattice, and changing the atomic positions by trial and error procedures. In the refinement, the least squares program "RADIEL" (10) was used. The atomic form factors and the anomalous dispersion terms were taken from the International Table (11). The intensity contribution by the 120 twins was estimated as about $1/50$, but was neglected in the present calculation.

The observed reflection data showed the monoclinic symmetry $F(h, k, l) \approx F(h, -k, l)$, and with few exceptions had extinction rules $h0l: l = 2n + 1$ and $0k0: k = 2n + 1$. These extinction rules suggest that the probable space group is $P2_1/c$; there are 108 metal atoms in the unit cell and 27 metal atoms in the asymmetric unit. With this space group, however, we could not obtain a reasonable solution which yields an R factor less than 0.24. We have, therefore, judged that the apparent space group $P2_1/c$ is false and that the extinction rule only means that the structure has local symmetries such as glide planes and screw axes; i.e., if an atom occupies a position (x, y, z) equivalent atoms occupy the positions such as $(x, y', z + 1/2)$ and $(x', y + 1/2, z')$. The data also showed that the hkl reflections with $h + k = 2n + 1$ are very weak; i.e., the crystal has a nearly C base centered symmetry (if this C centered symmetry is fulfilled, the unit cell will be reduced to the triclinic cell proposed by Zhou (5)).

At first, we have taken the space group $P1$. The positions of 108 metal atoms were refined, where the atoms were all assumed as Bi atoms with equal temperature factor. At this stage, the R factor was about 0.15. The positions of V atoms were deduced with the help of the difference Patterson maps which were calculated using the differences between the calculated and observed intensities. The obtained R factor was 0.10 when only metal atoms were taken into account and isotropic temperature factors were used. The number of adjustable parameters was 430. We have also examined the space group $P\bar{1}$. The R factor was 0.12, where the number of parameters was reduced to 217. According to the significance test program by Hamilton (12), the R factor ratio (≈ 1.2) suggests that the space group $P\bar{1}$ is rejected at the significance level of 0.01, but, it turned out that the structure refined with $P1$ did not satisfy the local symmetries mentioned above. Therefore, we have taken the latter space group $P\bar{1}$. The final atomic parameters are given in Table 2.¹

¹ A list of observed and calculated structure factors has been deposited with the National Auxiliary Publication Service. See NAPS document No. 05285 for 30 pages of supplementary materials. Order from ASIS/NAPS, Microfiche Publications, P.O. Box 3513, Grand Central Station, New York, NY 10163. Remit in advance \$4.00 for microfiche copy or for photocopy, \$7.75 up to 20 pages plus \$0.30 for each additional page. All orders must be prepaid. Institution and Organizations may order by purchase order. However, there is a billing and handling charge for this service of \$15. Foreign orders add \$4.50 for postage and handling, for the first 20 pages, and \$1.00 for additional 10 pages of materials, \$1.50 for postage of any microfiche order.

DESCRIPTION OF THE STRUCTURE
AND DISCUSSION

TABLE 2
Positional Parameters and Isotropic Thermal Parameters with
e.s.d.'s: Only the Positions of Metal Atoms Were Refined

Atom	X	Y	Z	U
V-01	0.2505(47)	0.1246(72)	0.1006(34)	0.029(17)
V-02	0.5700(28)	0.1112(46)	0.1143(21)	0.003(6)
Bi-03	-0.1161(9)	0.0978(15)	0.0947(8)	0.013(3)
Bi-04	0.0698(12)	0.2579(21)	0.0974(8)	0.032(6)
Bi-05	0.4004(7)	0.2934(12)	0.0845(5)	0.003(2)
Bi-06	-0.2679(9)	0.2795(13)	0.0963(6)	0.016(4)
Bi-07	0.2290(8)	0.4509(13)	0.0901(5)	0.013(3)
Bi-08	0.5480(8)	0.4543(13)	0.0711(5)	0.012(3)
Bi-09	-0.0949(21)	0.4227(29)	0.0800(13)	0.052(9)
V-10	0.0522(33)	0.5796(54)	0.0854(24)	0.003(10)
Bi-11	0.3812(8)	0.6294(10)	0.0908(5)	0.008(3)
V-12	-0.2683(33)	0.6071(49)	0.0766(24)	0.003(8)
Bi-13	0.2217(8)	-0.2230(13)	0.0804(6)	0.011(3)
Bi-14	0.5598(8)	-0.2473(13)	0.0867(5)	0.003(2)
Bi-15	-0.1069(15)	-0.2104(23)	0.0717(9)	0.041(7)
Bi-16	0.0603(7)	-0.0532(11)	0.0874(5)	0.002(2)
Bi-17	0.4040(10)	-0.0675(13)	0.0843(7)	0.002(3)
Bi-18	-0.2785(7)	-0.0566(10)	0.0719(5)	0.003(3)
Bi-19	0.1569(10)	0.1045(13)	0.2428(7)	0.004(3)
Bi-20	0.4974(9)	0.1149(14)	0.2421(6)	0.018(4)
Bi-21	-0.1531(9)	0.0974(15)	0.2626(6)	0.015(4)
Bi-22	0.3232(13)	0.2817(17)	0.2276(8)	0.020(4)
Bi-23	-0.3268(16)	0.2792(23)	0.2719(10)	0.032(7)
Bi-24	-0.0021(9)	0.2996(13)	0.2640(6)	0.021(3)
Bi-25	0.1724(11)	0.4339(17)	0.2578(7)	0.003(3)
Bi-26	0.5084(9)	0.4325(12)	0.2625(6)	0.015(3)
Bi-27	-0.1796(9)	0.4293(16)	0.2357(6)	0.015(4)
Bi-28	0.0026(8)	0.6157(13)	0.2579(6)	0.012(3)
Bi-29	0.3363(7)	0.5977(12)	0.2496(5)	0.005(3)
Bi-30	-0.3396(16)	0.5888(20)	0.2461(10)	0.031(7)
Bi-31	0.1776(11)	-0.2089(17)	0.2784(7)	0.021(5)
Bi-32	0.5004(8)	-0.2025(12)	0.2406(6)	0.016(3)
Bi-33	-0.1766(13)	-0.2063(17)	0.2192(8)	0.024(4)
Bi-34	0.3317(7)	-0.0703(12)	0.2475(5)	0.002(3)
Bi-35	-0.3256(21)	-0.0721(30)	0.2567(13)	0.036(7)
Bi-36	-0.0098(11)	-0.0679(15)	0.2340(7)	0.025(4)
Bi-37	0.1217(10)	0.1259(15)	0.4072(7)	0.022(4)
V-38	0.4387(31)	0.1094(47)	0.3867(22)	0.002(8)
V-39	-0.2351(114)	0.1505(177)	0.4483(75)	0.115(52)
Bi-40	0.2653(12)	0.2901(17)	0.4107(8)	0.031(5)
Bi-41	0.5993(7)	0.2887(12)	0.4145(5)	0.002(3)
Bi-42	-0.0603(6)	0.2543(10)	0.4179(4)	0.002(2)
Bi-43	0.0914(9)	0.4328(16)	0.4137(7)	0.011(4)
Bi-44	0.4519(10)	0.4501(17)	0.4294(6)	0.024(5)
Bi-45	-0.2301(26)	0.4394(45)	0.4145(18)	0.095(14)
V-46	0.2554(31)	0.6129(47)	0.4068(22)	0.003(9)
Bi-47	0.6132(9)	0.6055(12)	0.4085(7)	0.009(3)
V-48	-0.0786(62)	0.6188(99)	0.3984(44)	0.051(29)
Bi-49	0.1074(11)	-0.2076(17)	0.4278(7)	0.027(5)
Bi-50	0.4329(7)	-0.2450(11)	0.3995(5)	0.012(3)
Bi-51	-0.2210(7)	-0.2292(11)	0.4125(5)	0.005(3)
Bi-52	0.2782(7)	-0.0493(11)	0.4213(5)	0.003(2)
Bi-53	0.6010(13)	-0.0752(20)	0.4191(9)	0.025(6)
Bi-54	-0.0584(7)	-0.0481(11)	0.4148(5)	0.003(2)

The crystal is composed of six cation layers in the a - b plane, each containing 18 metal atoms. Figure 4 shows Fourier sections of the layers. The contours show the positions of the metal atoms; higher peaks correspond to Bi atoms and lower peaks to V atoms. Probably due to disorders described below, ambiguities exist about the positions of some V atoms. In the present analysis, we have set the number of vanadium atoms to $16 \approx 108 \times 1/7$. Figure 4 shows that V atoms form honeycomb lattices in the vanadium layers which contain V atoms. The stacking of the layers can be expressed by the numbers of V atoms, as 4-0-4-4-0-4. It will be compared with the trigonal arrangement, 0-0-6-0-0-6 found in the type I structure (Fig. 1).

The maps shown in Fig. 4 also disclose atomic displacements along the b axis; the atoms in the layers $z \approx 7/12$, $3/4$, and $11/12$ are shifted relatively to those in layers $z \approx 1/12$, $1/4$, and $5/12$. The displacements are not of the sinusoidal type but of the square wave type (see Fig. 5). Comparing the displacements (Fig. 5) and the atomic arrangements (Fig. 4), we can conclude that the large displacements are due to the Coulomb repulsion between the V atoms in the nearest neighbor sites. The cleavage in the a - b plane can also be attributed to the Coulomb repulsion between the vanadium layers.

These displacements ($\approx 0.6 \text{ \AA}$) can be compared with those of the martensitic phase transitions in ferrous alloys. The martensitic nature of the phase is also evident from the external appearance of the crystal (see Fig. 6). The phase sequence of the crystal may be as follows. When cooled from the molten state, it crystallizes first in the cubic fluorite structure (δ - Bi_2O_3) and has a disordered cation configuration. At the phase transition to the room temperature structure, in order to save the internal energy accompanying the large distortion ($\Delta\beta \approx -2.1^\circ$), the crystal takes a polysynthetic twin structure. At the twin boundary, as mentioned above, the axes a and b are rotated $+120^\circ$ or -120° . The honeycomb atomic arrangement in the vanadium layers will be convenient for the 120° twin formation. The lattice distortion is closely correlated with the arrangement of V atoms. Therefore, the phase transition from the δ phase will not be purely displacive (martensitic), but mixed with the order-disorder of cations.

The positions of oxygen atoms were searched for using the difference Fourier map, but suffered from ghosts due to the disorder of metal atoms; we could not determine the positions of oxygen atoms. Let us discuss the arrangement of oxygen atoms from another point of view. Recent structural studies have shown that V atoms have four coordination of oxygen atoms in the bismuth oxide system (5,

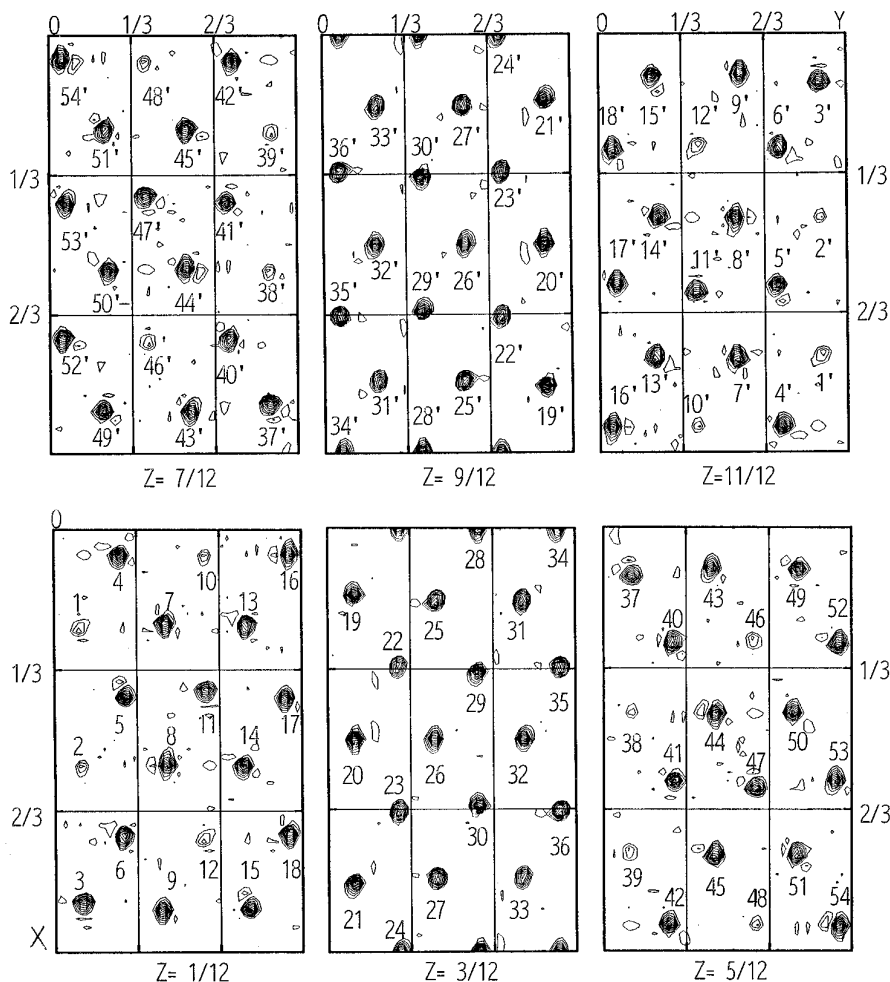


FIG. 4. Sections of the Fourier synthesis showing the positions of metal atoms (contours drawn in arbitrary units). The metal atoms are numbered; 1, 2, 10, 12, 38, 39, 46, and 48 are V atoms. Note that the atoms in the layers ($z \approx 1/12, 3/12,$ and $5/12$) are displaced along the b axis, relatively to those in layers ($z \approx 7/12, 9/12,$ and $11/12$). These displacements are attributed to the Coulomb repulsion between the V atoms in the nearest neighbor sites ($V2-V2', V10-V10', V39-V39',$ and $V48-V48'$).

8, 9). According to the analysis by Pauling (13), the ratio of atomic radii ($\gamma = r_V/r_O \approx 0.39$) is a decisive factor for the coordination number; if $\gamma < \sqrt{2} - 1$ fourfold coordination is stable. We will follow the analysis made by Zhou as to the coordination of V atoms in type I (5). There are $(108 - x)$ Bi atoms and x V atoms in the unit cell (here $x = 108 \times 1/7 \approx 15.4$); then oxygen atoms should number $162 + x \approx 177.4$ and anion vacancies should be $54 - x \approx 38.6$. If we assume there are no oxygen vacancies except for those surrounding V atoms, the number of vacancies around each V atom would be $38.6/15.4 \approx 2.5$. The Coulomb interaction will make V atoms separated as far as possible, while the coordination demand of V atoms and the number of available oxygen vacancies will make V atoms come to the nearest neighbor sites so that they share oxygen vacancies in common.

In the present structure, there are four $V_2O(v)_6$ and eight $VO(v)_4$ clusters (where O(v) represents the oxygen vacancy). This model will be compared with the tetrahedral V_4O_{10} or $V_4O(v)_{13}$ cluster model proposed by Zhou (5, 7). In recent Raman and NMR studies of the 6:1 compound done by Hardcastle *et al.* (8), the presence of tetrahedral V_4O_{10} clusters was excluded. They observed three crystallographically distinct V sites (each at $-492.7, -499.8,$ and -513.4 ppm in chemical shifts). The present structural data may suggest that the peak at -513.4 may be due to $V_2O(v)_6$ clusters, and the two peaks at -492.7 and -499.8 to $VO(v)_4$ clusters which have slightly different surroundings. The arrangement of oxygen vacancies will be tetrahedral, since the NMR spectra showed no quadrupole shift (8). The present model will require 16 V atoms and 56 oxygen vacancies ($4 V_2O(v)_6$ and $8 VO(v)_4$), but the number of avail-

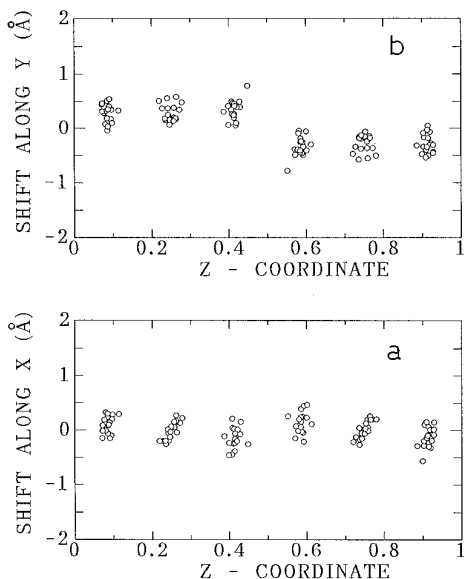


FIG. 5. Displacements of metal atoms from the positions in the prototypic cubic fluorite structure, (a) displacements along the a axis, (b) displacements along the b axis.

able oxygen vacancies is only 38. In order to determine the oxygen coordination, further detailed X-ray or preferably neutron diffraction data are desired.

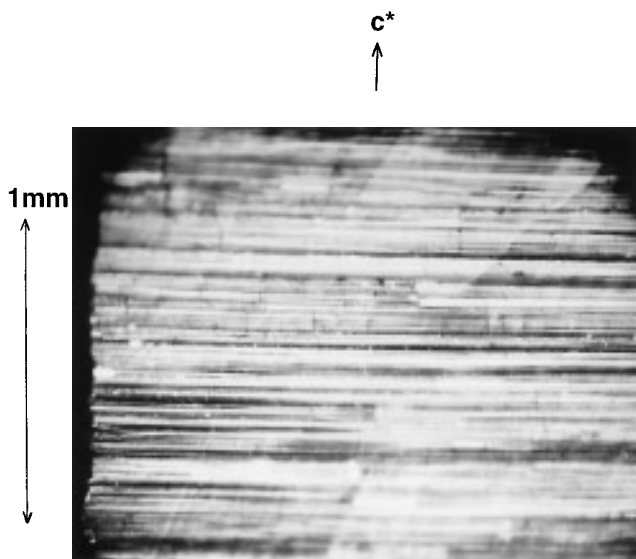


FIG. 6. The microphotograph of the crystal surface showing the multiple domain structure, view along the $[211]_c$ or the a axis.

In this study, the cation arrangements and their displacive nature of the 6:1 compound have been clarified. However, the quality of the data is not enough to determine the positions of oxygen atoms. Several difficulties are in the structure analysis. First, the atomic form factors of O ($Z = 8$) is much smaller than that of Bi ($Z = 83$). Second, the crystal has a large absorption coefficient and the used sample is a platelet, therefore, the geometrical correction for absorption may be incomplete. Third, the crystal inevitably contained a small amount of twins; the contamination of the diffraction intensities was ignored here. Fourth, the X-ray diffraction pattern shows strong diffuse streaks along the c^* axis. This means that the crystal has a large number of stacking faults in the c^* direction and disorders in the x and y coordinates.

As mentioned before, there is a small discrepancy between the formula unit used in the structure analysis ($23 \text{ Bi}_2\text{O}_3\text{-}4\text{V}_2\text{O}_5$) and the nominal composition of the sample ($6 \text{ Bi}_2\text{O}_3\text{-V}_2\text{O}_5$). A further thermodynamic investigation is now in progress to clarify this discrepancy and the phase transition mechanism.

ACKNOWLEDGMENTS

This work is supported in part by a Grant-in-Aid for Scientific Research on Priority Areas, "Dynamics of Fast Ions in Solids and its Evolution for Solid State Ionics," from the Ministry of Education, Science, and Culture, Japan.

REFERENCES

1. P. Conflant, J. C. Boivin, and D. Thomas, *J. Solid State Chem.* **35**, 192 (1980).
2. R. J. D. Tilley, *J. Solid State Chem.* **41**, 233 (1982).
3. W. Zhou, D. A. Jefferson, M. Alario-Franko, and J. M. Thomas, *J. Phys. Chem.* **91**, 512 (1987).
4. W. Zhou, D. A. Jefferson, and J. M. Thomas, *J. Solid State Chem.* **70**, 129 (1987).
5. W. Zhou, *J. Solid State Chem.* **76**, 290 (1988).
6. R. Miida and M. Tanaka, *Jpn. J. Appl. Phys.* **29**, 1132 (1990).
7. W. Zhou, *J. Solid State Chem.* **87**, 44 (1990).
8. F. D. Hardcastle, I. E. Wachs, H. Eckert, and D. A. Jefferson, *J. Solid State Chem.* **90**, 194 (1991).
9. S. Kashida, T. Hori, and K. Nakamura, *J. Phys. Soc. Jpn.* **63**, 4422 (1994).
10. P. Coppens, T. N. Guru Row, P. Leung, E. D. Stevens, P. J. Becker, and Y. W. Yang, *Acta Crystallogr. Sect. A* **35**, 63 (1979).
11. "International Tables for X-ray Crystallography" Vol. IV. Kynoch Press, Birmingham, 1974. [Present distributor Kluwer Academic Publishers, Dordrecht]
12. W. C. Hamilton, *Acta Crystallogr.* **8**, 502 (1965).
13. L. Pauling, "The Nature of the Chemical Bond," 3rd ed. Cornell Univ. Press, Ithaca, New York, 1960.